Journal of ELECTRONIC MATERIALS, Vol. 40, No. 5, 2011
DOI: 10.1007/s11664-010-1506-8

Thermoelectric Properties of SnO_2 Ceramics Doped with Sb and Zn

S. YANAGIYA,[1,2,3] N.V. NONG,[2] J. XU,[2] M. SONNE,[2] and N. PRYDS[2]

1.—Department of Electrical and Electronic Engineering, Hakodate National College of Technology, 14-1 Tokura, Hakodate, Hokkaido 042-8501, Japan. 2.—Fuel Cells and Solid State Chemistry Division, Risø National Laboratory for Sustainable Energy, Technical University of Denmark, 4000 Roskilde, Denmark. 3.—e-mail: yanagiya@hakodate-ct.ac.jp

Polycrystalline SnO_2-based samples ($Sn_{0.97-x}Sb_{0.03}Zn_xO_2$, x = 0, 0.01, 0.03) were prepared by solid-state reactions. The thermoelectric properties of SnO_2 doped with Sb and Zn were investigated from 300 K to 1100 K. X-ray diffraction (XRD) analysis revealed all XRD peaks of all the samples as identical to the rutile structure, except for the x = 0.03 sample, which had a small amount of Zn_2SbO_4 as a secondary phase. We found that the power factor of the x = 0.03 sample was significantly improved due to the simultaneous increase in the electrical conductivity and the Seebeck coefficient. A power factor value of $\sim 2 \times 10^{-4}$ W m^{-1} K^{-2} was obtained for the x = 0.03 sample at 1060 K, 126% higher than that for the undoped sample.

Key words: Oxide thermoelectric material, tin oxide, antimony, zinc, codoping

INTRODUCTION

Thermoelectric materials have attracted extensive interest in past decades as they can directly convert heat into electricity. Since Terasaki et al. reported that single-crystal $NaCo_2O_4$ shows a high power factor at 300 K,[1] oxide thermoelectric materials have been extensively studied.[2–4] Oxide-related materials with high performance are some of the most promising materials for thermoelectric devices because they are chemically and thermally stable at high temperature in air. The performance of a thermoelectric material at a given temperature T is determined by the dimensionless figure of merit $ZT = \sigma S^2 T \kappa^{-1}$, where σ, S, and κ represent the electrical conductivity, Seebeck coefficient, and thermal conductivity, respectively. For polycrystalline bulk materials, the ZT values of p-type $Ca_{2.7}Ag_{0.3}Co_4O_9$/Ag-10% composite[5] and n-type ZnO codoped with Al and Ga samples[6] were reported to be 0.5 at 1000 K and 0.65 at 1247 K, respectively. Considerable efforts have been made to increase ZT values further for various materials.

(Received May 8, 2010; accepted December 23, 2010; published online February 2, 2011)

Tin dioxide (SnO_2) crystallizes in a rutile-type structure with two equivalent a-axes (4.7382 Å) and a shorter c-axis (3.1871 Å),[7] and it has a wide band gap of 3.87 eV to 4.3 eV.[8] Stoichiometric pure SnO_2 is an insulator, while nonstoichiometric SnO_2 displays n-type conductivity due to oxygen vacancies or doping with elements such as antimony or fluorine.[8] For these reasons, the electrical conducting behavior of nonstoichiometric and impurity-doped SnO_2 has been studied for many years. Behr et al. reported that the electrical conductivity at room temperature for a 1 mol% Sb-doped polycrystalline pellet and a 0.1 mol% Sb-doped single crystal are 5.3 Ω^{-1} cm^{-1} and 48 Ω^{-1} cm^{-1}, respectively.[9] Because of its advantageous transport properties, doped SnO_2 can be used for transparent electrodes, solid-state gas sensors, and varistors. Because densification of SnO_2 ceramics without sintering aids is very difficult,[10] oxides such as CuO,[11] Bi_2O_3,[11] MnO_2,[11,12] CoO,[12] Co_2O_3,[13] Co_3O_4,[11,14,15] and $CaCO_3$[15] are used as sintering aids. On the other hand, Nb_2O_5,[8,14] La_2O_3,[12] Ta_2O_5,[13] Fe_2O_3,[14] Sb_2O_3,[15] and V_2O_5[16] can be used to control the electrical conductivity. Recently, Saadeddin et al. have reported that SnO_2 ceramics codoped with Sb^{5+} and Zn^{2+} showed a high electrical conductivity

and high density.[17] As for thermoelectric properties, Morgan and Wright measured the Seebeck effect in SnO_2 single crystals. The Seebeck coefficients ranged from approximately 50 μV K^{-1} to 220 μV K^{-1}, depending on the temperature or concentration of conduction electrons in the samples.[18] Tsubota et al. measured the thermoelectric behavior of SnO_2 ceramics doped with Ti and Sb up to 800°C and obtained the maximum figure of merit Z of 2.4×10^{-5} K^{-1} for the $Sn_{0.98}Ti_{0.01}Sb_{0.01}O_2$ sample.[19]

In this study, we synthesized polycrystalline $Sn_{0.97-x}Sb_{0.03}Zn_xO_2$ (x = 0, 0.01, 0.03) samples and characterized their thermoelectric properties. We found that the thermoelectric performance of SnO_2 can be improved by codoping with Sb and Zn.

EXPERIMENTAL PROCEDURES

Sb and Zn codoped SnO_2 ($Sn_{0.97-x}Sb_{0.03}Zn_xO_2$) polycrystalline solid solutions were prepared by a conventional solid-state reaction method. SnO_2 (99.9%), Sb_2O_5 (99.9998%), and ZnO_2 (99.99%) powders were used as starting materials. The powders were weighed, mixed, and ball-milled in ethanol for 24 h. After milling, the powders were pressed with a cold isostatic press at 250 MPa. Finally, the samples were sintered at 1573 K for 10 h in flowing air with a heating and cooling rate of 2 K min^{-1}. The crystalline structure properties of the samples were studied by x-ray diffraction (XRD) using a Bruker D8 diffractometer with Cu K_α radiation. The microstructure of the fractured surface of the samples was observed with a Hitachi scanning electron microscope (SEM) TM-1000. The densities of the samples were evaluated by measuring the volume and weight of the samples with a digital micrometer and a digital balance. The high-temperature electrical conductivity and the Seebeck coefficient were simultaneously measured using an ULVAC-ZEM3 device under a low-pressure helium atmosphere. The thermal conductivity was measured by a laser flash technique using a Netzsch LFA-457 in a nitrogen atmosphere.

RESULTS AND DISCUSSION

Figure 1 shows XRD patterns of undoped SnO_2 and $Sn_{0.97-x}Sb_{0.03}Zn_xO_2$ (x = 0, 0.01, 0.03) ceramics. It can be seen that all the samples except the x = 0.03 sample were composed of a single-phase compound with a rutile structure. Four weak peaks observed in the XRD pattern for the x = 0.03 sample were attributed to the diffraction peaks of the secondary phase Zn_2SnO_4. Our results indicated the solubility limit of Zn in SnO_2 doped with 3 at.% Sb to be less than 3 at.%.

Figure 2 shows SEM images of undoped SnO_2 and $Sn_{0.97-x}Sb_{0.03}Zn_xO_2$ (x = 0, 0.01, 0.03) ceramics. The densities of the samples were 4.08 g cm^{-3}, 3.90 g cm^{-3}, 4.19 g cm^{-3}, and 5.45 g cm^{-3}, respectively. The undoped SnO_2 consisted of agglomerated

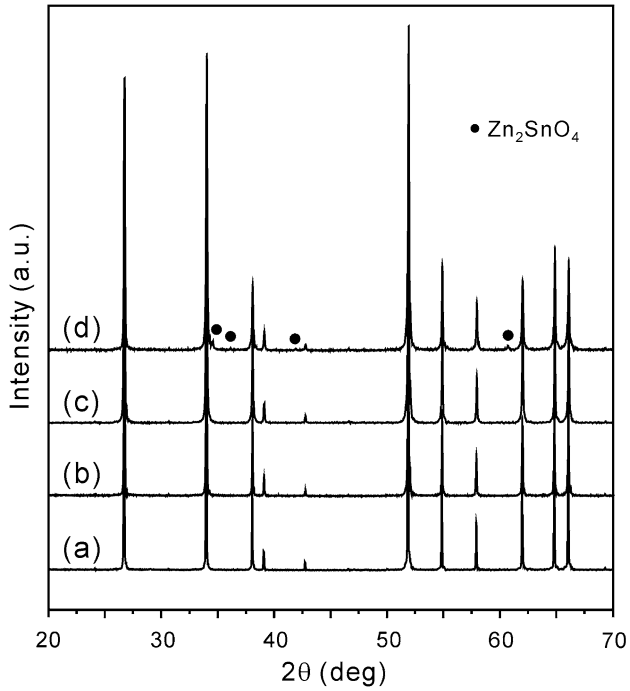

Fig. 1. XRD patterns of undoped SnO_2 and $Sn_{0.97-x}Sb_{0.03}Zn_xO_2$ ceramics: (a) undoped SnO_2, (b) x = 0, (c) x = 0.01, and (d) x = 0.03.

particles with diameters ranging from sub-μm to approximately 5 μm, and many pores were observed. Doping with 3 at.% Sb led to a decrease in the density and grain size of SnO_2. This is due to the fact that the doping of Sb_2O_3 decreases the concentration of oxygen vacancies, resulting in reduced mass transport.[11] On the contrary, doping with Zn significantly increased the grain size of SnO_2, as shown in Fig. 2c, d. It can be seen that facets between grains developed as the amount of Zn doping increased. This result clearly shows that Zn doping enhanced mass transport at the grain boundaries.

The temperature dependence of the electrical conductivity of the samples is shown in Fig. 3. The electrical conductivity of the undoped SnO_2 sample increased with increasing temperature and reached a nearly constant value at temperatures above 700 K. Doping with Sb significantly enhanced the electrical conductivity, indicating that Sb doping introduced free electrons in the conduction band. For the x = 0 sample, the electrical conductivity increased with temperature and reached the maximum value of 280 Ω^{-1} cm^{-1} at approximately 620 K, and then decreased as the temperature was increased. It is interesting that the x = 0.03 sample showed the highest electrical conductivity among the samples at high temperatures. The behavior of the electrical conductivity of the samples with different doping levels and morphology can be explained by considering the following competing factors: (1) Zn doping leads to an increase in the density and the grain size, which increases the time

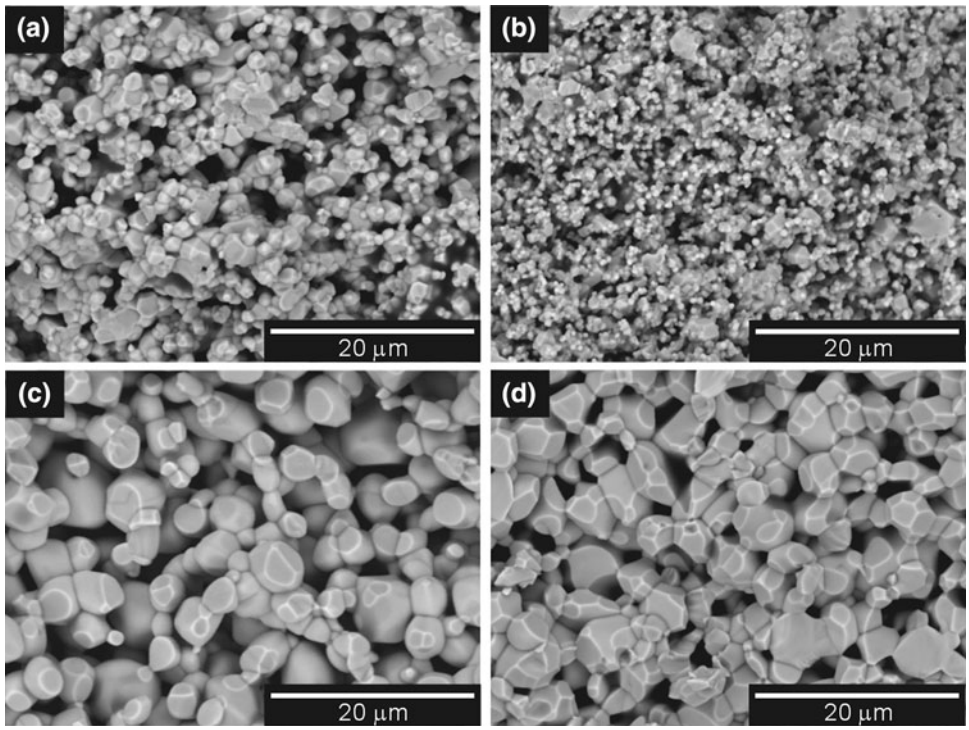

Fig. 2. SEM images of undoped SnO_2 and $Sn_{0.97-x}Sb_{0.03}Zn_xO_2$ ceramics: (a) undoped SnO_2, (b) $x = 0$, (c) $x = 0.01$, and (d) $x = 0.03$.

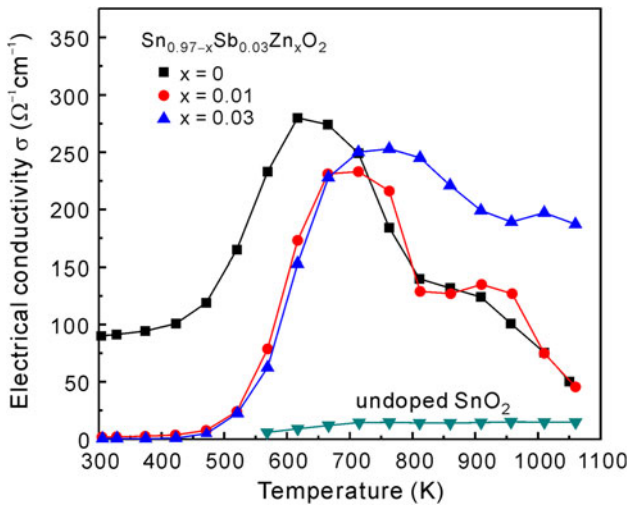

Fig. 3. Temperature dependence of the electrical conductivity of the samples.

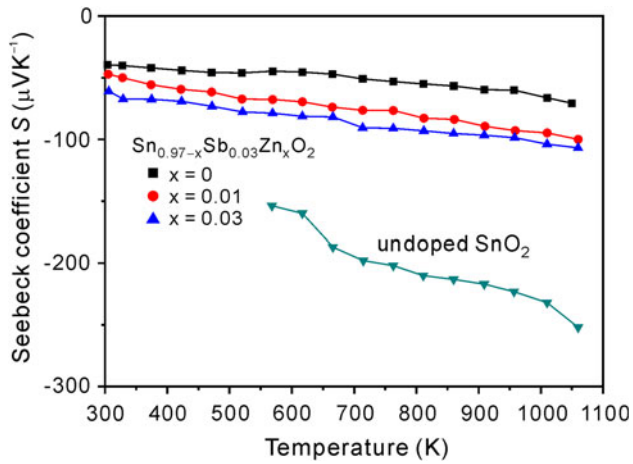

Fig. 4. Seebeck coefficient as a function of temperature for the samples.

between electron scattering events of charge carriers, and thus increases electrical conductivity. (2) Zn doping of SnO_2 leads to an increase in carrier mobility,[17] which also increases the electrical conductivity. (3) Substitution of Zn^{2+} for Sn^{4+} increases the hole concentration of the system, leading to a decrease in the electron concentration and thus a decrease in the electrical conductivity.[20] It is considered that, for the $x = 0.03$ sample, factors 1 and 2 dominantly affect the electrical conductivity, compared with factor 3. Further investigation is needed to clarify the effect of Zn doping on the electrical conductivity of SnO_2.

The temperature dependence of the Seebeck coefficient of the samples is displayed in Fig. 4. All the samples have negative Seebeck coefficients, indicating that a majority of carriers are electrons. The Seebeck coefficient of all the samples gradually increased with increasing temperature. The absolute values of the Seebeck coefficient for the undoped SnO_2 ranged from 150 $\mu V\ K^{-1}$ to 250 $\mu V\ K^{-1}$. The absolute values of the Seebeck coefficient for the Sb-doped samples were lower

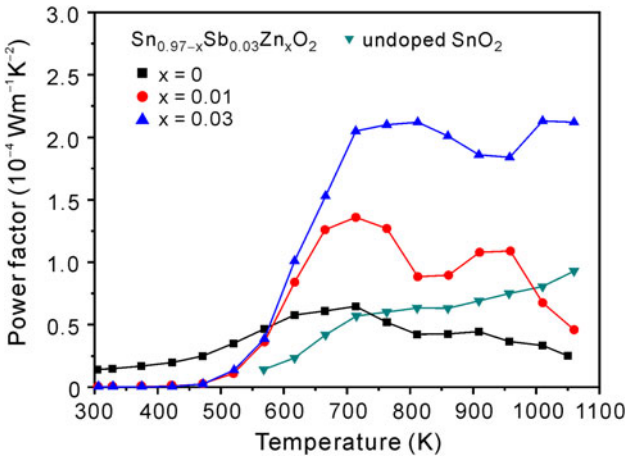

Fig. 5. Temperature dependence of the power factor of the samples.

than those of the undoped samples, which is in agreement with the results shown by Tsubota et al.[19] Note that the absolute values of the Seebeck coefficient were enhanced for the samples codoped with Sb and Zn. The $x = 0.03$ sample showed higher absolute values of the Seebeck coefficient than those of the $x = 0.01$ sample over the entire temperature range. In general, the value of the Seebeck coefficient decreases with increasing carrier density in common semiconductors.[21] The decrease in carrier concentration by Zn doping is probably related to the increase in the Seebeck coefficient. Our results also indicate that the influence of grain size on the Seebeck coefficient of SnO_2 is small.

Figure 5 presents the temperature dependence of the power factor. While the values of the power factor for the undoped SnO_2 and the $x = 0$ samples were mostly below 1×10^{-4} W m^{-1} K^{-2} over the measured temperature range, those for the samples codoped with Sb and Zn were higher. The maximum power factor (2.13×10^{-4} W m^{-1} K^{-2}) was obtained for the $x = 0.03$ sample at 1060 K. Improvement of the power factor could be expected through optimization of the doping levels of Sb and Zn.

CONCLUSIONS

We have prepared SnO_2 ceramics simultaneously doped with Sb and Zn ($Sn_{0.97-x}Sb_{0.03}Zn_xO_2$, $x = 0$, 0.01, 0.03) by solid-state reaction. XRD analysis revealed that the samples with $x = 0$ and 0.01 showed a single-phase rutile structure, while the $x = 0.03$ sample contained a small amount of Zn_2SbO_4 as a secondary phase along with the main phase of SnO_2. Simultaneous doping with Sb and Zn increased the grain size and the density. We found an increase in both the electrical conductivity and the absolute value of the Seebeck coefficient for the codoped sample with $x = 0.03$ above 700 K compared with those for the sample doped with only Sb. The increased electrical conductivity should be due to the enhanced grain growth and the increase in carrier mobility by Zn doping. The increase in the Seebeck coefficient is probably due to the decrease in carrier concentration by Zn doping. The influence of grain size on the Seebeck coefficient of SnO_2 was small. The maximum power factor value of approximately 2×10^{-4} W m^{-1} K^{-2} was obtained for the $x = 0.03$ sample at 1060 K.

REFERENCES

1. I. Terasaki, Y. Sasago, and K. Uchinokura, *Phys. Rev. B* 56, R12685 (1997). doi:10.1103/PhysRevB.56.R12685.
2. R. Funahashi, I. Matsubara, H. Ikuta, T. Takeuchi, U. Mizutani, and S. Sodeoka, *Jpn. J. Appl. Phys.* 39, L1127 (2000). doi:10.1143/JJAP.39.L1127.
3. H. Muta, K. Kurosaki, and S. Yamanaka, *J. Alloys Compd.* 350, 292 (2003). doi:10.1063/1.1847723.
4. T. Tsubota, M. Ohtaki, K. Eguchi, and H. Arai, *J. Mater. Chem.* 8, 409 (1998). doi:10.1039/a706213c.
5. Y. Wang, Y. Sui, J. Cheng, X. Wang, and W. Su, *J. Alloys Compd.* 477, 817 (2009). doi:10.1016/j.jallcom.2008.10.162.
6. M. Ohtaki, K. Arai, and K. Yamamoto, *J. Electron. Mater.* 38, 1234 (2009). doi:10.1007/s11664-009-0816-1.
7. G.J. McCarthy and J.M. Welton, *Powder Diffract.* 4, 156 (1989).
8. K.L. Chopra, S. Major, and D.K. Pandya, *Thin Solid Films* 102, 1 (1983). doi:10.1016/0040-6090(83)90256-0.
9. G. Behr, G. Krabbes, J. Werner, P. Dordor, and J.-P. Doumerc, *Phys Stat. Sol. (a)* 118, K91 (1990). doi: 10.1002/pssa.2211180238.
10. T. Kimura, S. Inada, and T. Yamaguchi, *J. Mater. Sci.* 24, 220 (1989). doi:10.1007/BF00660957.
11. M.S. Castro and C.M. Aldao, *J. Euro. Ceram. Soc.* 18, 2233 (1998). doi:10.1016/S0955-2219(97)00130-1.
12. M.R. Cássia-Santos, V.C. Souza, M.M. Oliveira, F.R. Sensato, W.K. Bacelar, J.W. Gomes, E. Longo, E.R. Leite, and J.A. Varela, *Mater. Chem. Phys.* 90, 1 (2005). doi: 10.1016/j.matchemphys.2003.12.014.
13. G.-Z. Zhang, J.-F. Wang, H.-C. Chen, W.-B. Su, C.-M. Wang, and P. Qi, *J. Phys. D Appl. Phys.* 38, 1072 (2005).
14. R. Parra, C.M. Aldao, J.A. Varela, and M.S. Castro, *J. Electroceram.* 14, 149 (2005). doi:10.1007/s10832-005-0879-1.
15. J.A. Aguilar-Martínez, M.B. Hernández, A.B. Glot, and M.I. Pech-Canul, *J. Phys. D Appl. Phys.* 40, 7097 (2007). doi: 10.1088/0022-3727/40/22/035.
16. A.V. Gaponov, A.B. Glot, A.I. Ivon, A.M. Chack, and G. Jimenez-Santana, *Mater. Sci. Eng. B* 145, 76 (2007). doi: 10.1016/j.mseb.2007.10.003.
17. I. Saadeddin, H.S. Hilal, B. Pecquenard, J. Marcus, A. Mansouri, C. Labrugere, M.A. Subramanian, and G. Campet, *Solid State Sci.* 8, 7 (2006). doi:10.1016/j.solidstatesciences.2005.09.002.
18. D.F. Morgan and D.A. Wright, *Br. J. Appl. Phys.* 17, 337 (1966). doi:10.1088/0508-3443/17/3/305.
19. T. Tsubota, T. Ohno, N. Shiraishi, and Y. Miyazaki, *J. Alloys Compd.* 463, 288 (2008). doi:10.1016/j.jallcom.2007.09.001.
20. J.-H. Yu and G.M. Choi, *Sens. Actuators B* 52, 251 (1998). doi:10.1016/S0925-4005(98)00275-5.
21. C.M. Bhandari and D.M. Rowe, *CRC Handbook of Thermoelectrics* (Boca Raton: CRC Press, 1995).